

Robustness of a state with Ising topological order against local projective measurements

Sanjeev Kumar and Vikram Tripathi

*Department of Theoretical Physics, Tata Institute of Fundamental Research,
Homi Bhabha Road, Navy Nagar, Mumbai 400005, India*

(Dated: March 13, 2024)

We investigate the fragility of a topologically ordered state, namely, the ground state of a weakly Zeeman perturbed honeycomb Kitaev model to environment induced decoherence effects mimicked by random local projective measurements. Our findings show the nonabelian Ising topological order, as quantified by a tripartite mutual information (the topological entanglement entropy γ), is resilient to such disturbances. Further, γ is found to evolve smoothly from a topologically ordered state to a distribution of trivial states as a function of rate of measurement (temperature). We assess our model by contrasting it with the Toric Code limit of the Kitaev model, whose ground state has abelian Z_2 topological order, and which has garnered greater attention in the literature of fault-tolerant quantum computation. The findings reveal the topological order in the Toric Code limit collapses rapidly as opposed to our model where it can withstand higher measurement rates.

I. INTRODUCTION

Topologically ordered states are a fascinating class of quantum states that exhibit exotic properties such as edge modes, anyonic excitations, and long-range entanglement. These states have the potential to revolutionize quantum information processing and computing. However, their practical use may be hindered by the susceptibility of these states to errors and decoherence. Measurements induce errors in a topologically ordered state, and understanding the effects of these errors on the state's properties is essential for the development of robust quantum technologies. Owing to this, the interplay of projective measurements and topological order is a topic of current research interest [1, 2]. In this work, we investigate the robustness of topologically ordered states against local projective measurements. We explore the aftermath of such measurements on the state's entanglement properties. Our results provide insights into the mechanisms that enable the resilience of topologically ordered states against local measurements.

From preparation of a quantum state to its characterization, local projective measurements are an indispensable tool for tweaking quantum many-body systems and thereby exploring the rich physics offered by them [3–8]. A well-prepared quantum system is typically prone to decoherence due to coupling with its environment. A recent study [9] smoothly bridges the impact of weak continuous disturbance on a quantum many body system with the discrete measurements being performed on it. Here, we mimic the environmental impact on a quantum system through spatially-random local projective measurements on the system. The rate of such random measurements will thus correspond to the temperature of the environment.

The literature reveals findings of measurement-induced phase transitions [10–19] in short-range interacting models. Ergodic systems undergo a transition from volume-law states to steady states having an area-law entanglement entropy. Efforts are made to see similar effect in

long-range models as well [20–26], where typically due to quick building of entanglement, the saturating entanglement entropy is still proportional to the system size. The effect of local measurements has also been studied for area-law states in 1D noninteracting fermion hopping models [27], and a measurement induced transition between states of differing ground state degeneracy has been observed. In this study we are interested in two dimensional systems where the initial state possesses topological order. For being able to alter the entanglement structure of steady states and possible applications of such states in Quantum Information to engineering dynamical phases of matter, the field has acquired much attention. We concern ourselves with the ground state of the 2D isotropic Kitaev Hamiltonian [28]. The excitations are fractionalized quasiparticles – free Majorana fermions and gapped half-vortices (visons). More importantly, the short-range model exhibits Z_2 topological order [29]. One manifestation of this topological order is that the bipartite von Neumann entanglement entropy is smaller than the expected area law by a constant amount $\gamma = \ln 2$ known as the topological entanglement entropy (TEE). Adding a small Zeeman field results in a state with Ising topological order (ITO) with the same value of $\gamma = \ln 2$. The field also opens a bulk gap for the Majorana fermions. For fields B exceeding a few per cent of the Kitaev interaction J (e.g. $B/J \approx 0.025$ with ferromagnetic Kitaev interactions and $\mathbf{B} = B(111)$), ITO is lost [30, 31]. The gap also provides protection against thermal excitations. We study the interplay between disentangling measurements and entanglement building unitary evolution and show it results in steady states with finite γ . We further compare our results with the Toric Code model which is well-known in the literature of fault-tolerant quantum computation and whose ground state possess Z_2 topological order with the same $\gamma = \ln 2$ as ITO. Such a state has recently been prepared using a specific protocol of projective measurements on real quantum hardware [32]. We find entanglement of the latter is significantly more fragile against random local projective

measurements.

The remaining sections of the paper are structured as follows: In Sec. II, we present our model and outline the measurement protocol. Section III focuses on presenting results, specifically highlighting the dynamics of TEE. Additionally, this section delves into the diagnosis of the topologically ordered state through local projective measurements. Finally, Sec. IV provides a summary of our findings and includes a discussion.

II. MEASUREMENT ROUTINE

We consider the following Hamiltonian,

$$\hat{H} = - \sum_{\langle ij \rangle_{\eta\text{-link}}} \sigma_i^\eta \sigma_j^\eta + B \sum_{i,\eta} \sigma_i^\eta, \quad (1)$$

where the first term on the RHS is an isotropic ferromagnetic Kitaev interaction on the honeycomb lattice. Here i labels the spin-1/2 degrees of freedom on the lattice and $\langle ij \rangle_{\eta\text{-link}}$ denotes the nearest neighbors i, j on the three types of links labeled $\eta = x, y, z$. The second term on the RHS is a coupling to an external Zeeman field in $(1, 1, 1)$ direction. We set the Kitaev interaction strength to unity and external magnetic field, $B = 0.01$, which places the ground state well within the ITO phase. We confirmed that the small magnetic field preserves the TEE, which we obtained using the Kitaev-Preskill construction [29]. We initialize the system in the ground state of the Hamiltonian, Eq. (1). The decoherence is introduced via periodically timed local projective measurements on randomly chosen qubits. The protocol for carrying out the measurement is described below.

We consider a system undergoing N measurements at equally spaced intervals over a duration τ . Each measurement involves selecting a lattice site i from a uniform distribution over $1, 2, \dots, L$, where L denotes the system size. At each chosen site, a local projection operator acts. We consider the following spin-up and spin-down projection operators respectively:

$$\mathcal{P}^\pm = \frac{1 \pm \sigma_i^z}{2}. \quad (2)$$

The projection operator on the i^{th} -spin is defined as

$$\mathcal{P}_i = p\mathcal{P}^+ + (1-p)\mathcal{P}^-, \quad (3)$$

where we determine the choice of p (either 0 or 1) by comparing the expectation value of σ_i^z in the instantaneous state at the time of measurement with a uniformly drawn number c from the interval $(-1, 1)$. For state $|\Psi\rangle$, satisfying the condition $\langle \Psi | \sigma_i^z | \Psi \rangle > c$ we impose $p = 1$ and project the state onto the subspace-I where the i^{th} -spin is up. Otherwise, $p = 0$ and we project onto the spin-down subspace-II as shown in Fig. (1). The rationale for introducing the comparison with a random number is to incorporate the inherent quantum mechanical probabilities of both possible measurement outcomes for the

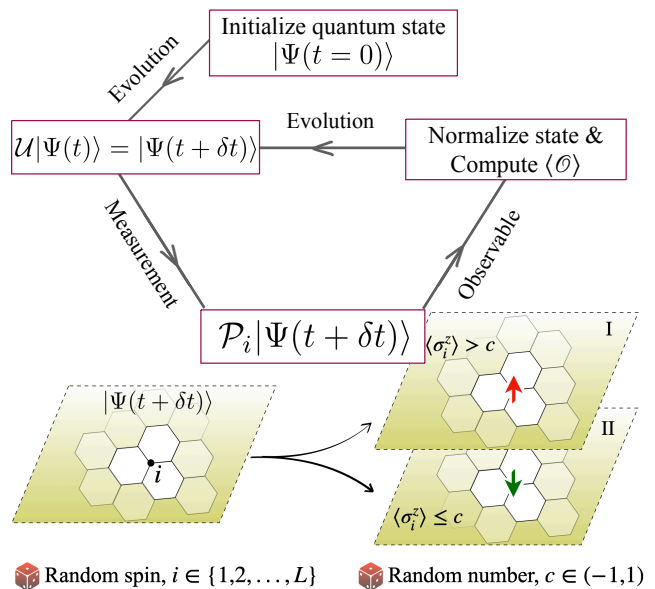


Figure 1. Flowchart depicting the measurement protocol: The system is initialized in a topologically ordered ground state, $|\psi(0)\rangle$, and unitarily evolved under the Hamiltonian Eq. (1). A local measurement operator, \mathcal{P}_i selects a spin i from a uniform distribution over the integers from 1 through L , projecting the quantum state onto either of the shown subspaces depending on the $\langle \sigma_i^z \rangle$ and its comparison with a real number c sampled from a uniform distribution in $(-1, 1)$. The quantum state projection is normalized and observables' expectation $\langle \mathcal{O} \rangle$ are computed. The observables are self-averaged over $n \gg 1$ runs. Here, $\delta t = \tau/N$ and N is the number of local projections made periodically (stroboscopically) in the duration τ .

state $|\Psi\rangle$, even in single-shot measurements. Simply determining the outcome based solely on the expectation value $\langle \Psi | \sigma_i^z | \Psi \rangle$ (being greater or less than zero) would not capture the finite probability of obtaining the less likely outcome. This comparison with c , therefore, serves as a probabilistic mechanism to select the appropriate subspace. This approach also mimics the actual experimental situation, where each measurement yields a pure state, which subsequently becomes the starting point for the next evolution cycle. Following the measurement, we normalize the obtained quantum state (either I or II) and calculate expectation values of observables. These expectations are then self-averaged over a large number of runs ($n \gg 1$). Notably, incorporating a random number in this manner bears resemblance to the Metropolis algorithm and presents an alternative strategy for non-unitary stochastic state evolution, circumventing the need for the density matrix formalism (see also [33]). Investigation of decoherence induced by random local projections has been studied without the random number approach and specifically using a deterministic criteria wherein each qubit in a one-dimensional quantum Ising chain model was periodically probed with a homogeneous probability [34].

The unitary evolution attempts to heal the entanglement structure following a projective measurement. Any particular realization of N measurements on a system of L qubits (spins) will traverse one from the total of $n = L^N$ possible trajectories. However, keeping track of exponentially large number of trajectories may not be the plausible choice; for many observables show self-averaging and quickly reach a steady state value even when averaged over few ($n \gg 1$) typical paths. This in fact is the situation in our simulations. We keep track of the saturation (i.e. steady state) value dependence on various measurement rates and duration of the protocols. Our analysis reveals the emergence of non-equilibrium steady state (NESS) in Kitaev system. We find a smooth transition from the ground state, which is a non-trivial state to a trivial state as the measurement rate (temperature) is increased. However, the exponential decay to the topologically trivial state is much slower when compared to the anisotropic Kitaev model,

$$\hat{H} = - \sum_{\langle ij \rangle_{\eta\text{-link}}} J^\eta \sigma_i^\eta \sigma_j^\eta, \quad (4)$$

in the Toric Code limit $|J^z| > |J^x| + |J^y|$. We explore the behavior of both the models in the following section.

III. RESULTS

As the system is disturbed periodically, we would like to inquire the manner in which a gapped topologically robust quantum system decoheres. Signature for the same can be captured in entanglement entropy and mutual information [35–42]. We first study the entanglement entropy on account of repeated measurement on randomly chosen qubits of the system. The Kitaev ground state is associated with a finite TEE, which is the part of the von Neumann bipartite entropy, $S_A = -\text{Tr} \rho_A \log \rho_A = \alpha L - \gamma$, remaining after subtracting the area law contribution. Here L is the perimeter of a 2D subsystem A whose bipartite entanglement entropy is S_A . For the Kitaev ground state, $\gamma = \ln 2$. We numerically obtain γ using the well-known Kitaev-Preskill construction [29, 31]. Ground states are obtained through exact diagonalization for a system size of up to $L = 24$. The simulation of non-unitary stochastic evolution is conducted using QUSPIN [43, 44]. Note that S_A , being a non-linear function of ρ_A yields two possibilities for averaging over $n \gg 1$ trajectories (measurement histories), namely $\overline{S_A}(\rho_A)$ or $S_A(\overline{\rho_A})$. We consider the former alternative, for it includes solely the quantum correlations [45].

In Fig. 2, we show the time-dependence of γ for several measurement rates. All the curves begin at the ground state of Kitaev Hamiltonian in the presence of small Zeeman field. As periodic measurements are done on the system, the TEE falls. For lower rates of measurement, the unitary evolution gets enough time to build-up the entanglement and hence, the system is able to revive the

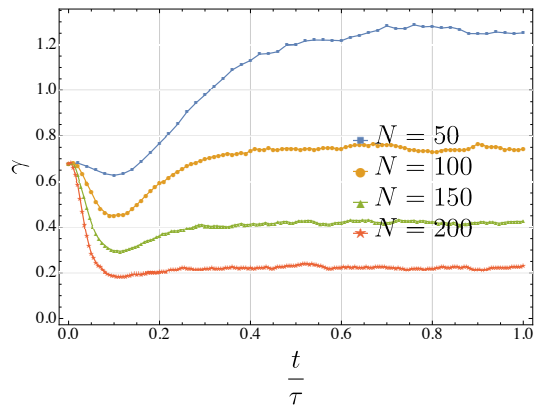


Figure 2. Time evolution of TEE, γ for different rates of measurement. We begin with the ground state of Eq. (1) for the system size, $L = 16$. N is the total number of measurements made periodically in time $\tau = 10J^{-1}$. We have set $\hbar = 1$. A total of thousand realizations (n) are averaged over to obtain the plots. The fall and then rise of γ at lower N results from the intricate play of projective measurements and entanglement building, unitary evolution. For higher N , the disruptive measurements impede the resurgence of mutual information.

tripartite mutual information. Saturation values, γ_s are obtained towards the end of the protocol in Fig. 2, which drop monotonically with the rate of measurement (per site), $r = \frac{N}{\tau L}$.

A. Non-Equilibrium Steady State

Focusing on Fig. 2 we anticipate the establishment of a NESS. Figure 3, clearly pictures the NESS. At any given rate of measurement, a steady tripartite mutual information is established. As shown in Fig. 3, for the Kitaev system in the ITO phase, the saturation values of TEE follow an exponential decay after attaining an initial short time peak.

Inspection of the saturation values of TEE as a function of rate of measurement illustrates the relative robustness of γ in the Kitaev system as opposed to the comparable Toric Code model (see Fig. 4) which has an abelian Z_2 topological order and the same value $\gamma = \ln 2$ for the TEE. At small temperatures, the quantum system is superposed in a state of higher tripartite mutual information. However, in the latter model, γ rapidly collapses to zero numerically even for a small rate of measurement. When examining mutual information at nonzero measurement rates, the comparison distinctly demarcates the two models. The loss of topological order in Toric Code at any finite temperature has been attributed to vison excitations [46] in the literature. For comparable energy densities, the Toric Code limit of the Kitaev model has a smaller vison gap than its Kitaev counterpart. However the Majorana gap is much smaller in the Kitaev ITO

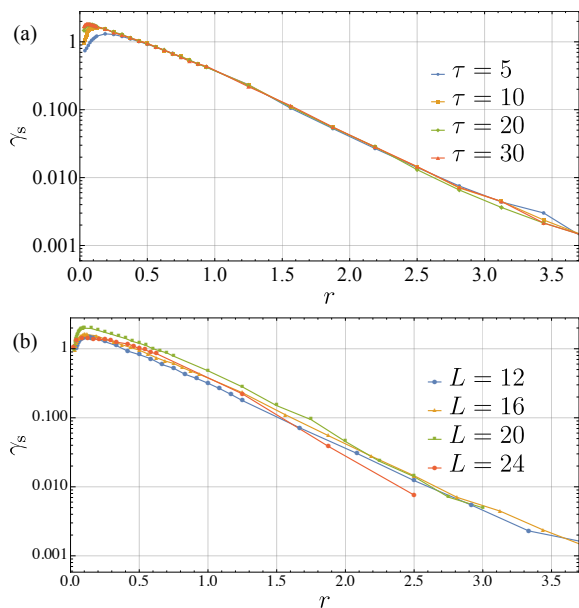


Figure 3. Saturation values of TEE, γ_s for a Kitaev system subjected to a small Zeeman field $\mathbf{B} = 0.01J(111)$ are plotted as obtained after a rate of measurement, r . Overlapping regions of various time duration τ protocols in (a) highlight the establishment of NESS in an $L = 16$ -site system. (b) displays γ_s for different system sizes with $\tau = 10J^{-1}$. We see an exponential decay after a peak. The initial difference in the peaks can be attributed to the ground state energy gap in various sizes. The decay however, is indifferent to system sizes.

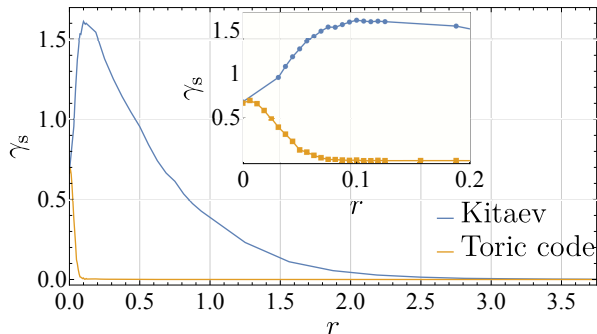


Figure 4. Comparison of the TEE as withheld by the Kitaev system, Eq. (1) and Toric Code model, Eq. (4) is shown. Despite the same initial TEE, the latter model shows rapid decline of the γ_s . Plots are for the system size $L = 16$ and protocol duration $\tau = 10J^{-1}$. For the Toric Code, $J^x = J^y = 10^{-1}J^z$, such that the ground state energies per site is same for both the models. Inset displays the behavior at small rates of measurement.

phase than in the Toric Code phase. This indicates the strong dependence of the TEE on the gauge sector.

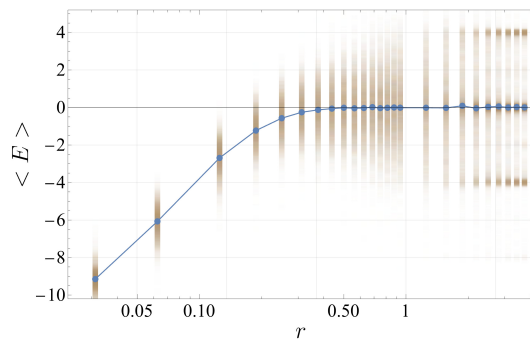


Figure 5. Energy expectation $\langle E \rangle$ as obtained for the Kitaev system, Eq. (1) with $L = 16$ and $\tau = 10J^{-1}$ at different measurement rates r is shown. Each blue-colored point is an average of $n = 5000$ brown-colored squares distributed vertically around it. The latter corresponds to different realizations at r . We see a clear distinction of energy sectors whose superposition result in the non-vanishing tripartite mutual information. At higher r , this distinction becomes prominent, though, on account of large number of projective measurements, the state has vanishing γ (see Fig. 2). The entire spectrum lies in the range $\pm 13.4J$.

B. Diagnosis of Topological Order

To delve into what exciting superposition the Kitaev system goes through to yield non-vanishing mutual information, we examine the expectation values of the Hamiltonian at different rates of random projective measurements, Fig. 5. Owing to randomness, a given rate of measurement r in each realization yields, in general, different energy expectation. Each yellow dot in Fig. 5 represents the energy of the quantum state at the end of the measurement protocol for an individual run and averaging over these values gives the curve with the blue dots. Notably, at higher rates of measurement, the energy distribution has multiple peaks, which is clearly not thermal. The peak at the centre of the spectrum $E = 0$ has approximately 50% weight, and is flanked by two more side peaks ($E = \pm 4$ in the figure) with approximately a quarter weight each. Such structure is not seen for small r .

Remarkably, even in the high measurement rate regime, signatures of the initial topologically ordered state continue to persist. Rapid random projections prohibit state evolution and act as snapshot of the initial state from different directions in the Hilbert space. Figure 6 illustrates the distribution of total magnetization $M_z = \sum_i \sigma_i^z$ as obtained after the establishment of the steady state for $r = 3.75$ in different models when starting from their respective ground states.

We see clear diagnosis of the topologically ordered states, namely, the ground state of Kitaev and Toric Code model. In these two cases, the magnetization distribution shows a number of sharp peaks uniformly separated by steps of two spin flips (bimagnons) around the mean zero magnetization. In Ising model, we get a continuous dis-

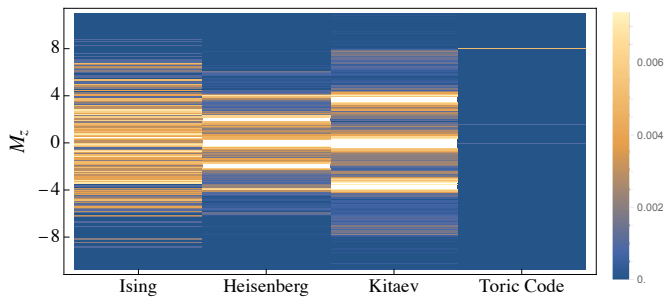


Figure 6. Statistical distribution of magnetization $M_z = \sum_i \sigma_i^z$ as obtained in different models for the rate of measurement, $r = 3.75$. We have $L = 16$ for all the models on a 2D honeycomb lattice. Ising(xx), Heisenberg and Kitaev correspond to the Hamiltonians with coupling strength of unity in the presence of a small Zeeman field $\mathbf{B} = 0.01J(111)$. For the Toric Code limit of the Kitaev model, we have chosen $J^x = J^y = 10^{-1}J^z$. In the case of the topologically ordered Kitaev and Toric Code states, distinct bimagnon peaks are seen at $M_z = 0, \pm 4, \dots$ while in the Ising model a continuous distribution, and in the Heisenberg case, single magnon peaks are seen.

tribution while in Heisenberg model, magnetization separated by a single magnon flip (± 2 units) is seen. Owing to the σ^z -projective measurements, the statistical distribution of M_x and M_y shows a continuous spread around 0 magnetization in Kitaev and Toric Code model.

IV. DISCUSSIONS

The interplay of entanglement building, unitary evolution and decohering effect brought about by random projective measurements on the topological orders of an ITO and Z_2 ordered state respectively are studied. The initial and final states in this case are both area-law

type and the transition is in their topological properties. In contrast, in typical volume-law states, a sharp measurement-induced phase transition to area-law states as a function of rate of measurement is seen. In the case of the Kitaev Hamiltonian ground state in the presence of tiny Zeeman field, we found an exponential decline (with measurement rate) of the TEE of the final state to a non-ergodic trivial state. A similar decohering protocol applied to the Toric Code limit of the Kitaev model reveals that the topological order in the latter is much more fragile. Earlier studies have suggested the role of vison excitations in the loss of Z_2 topological order of the Toric Code at any non-zero temperature [46]. We found that even at high rates of projective measurement, the magnetization distribution retains distinct signatures of the initial topological order in the form of highly excited bimagnon states around $M_z = 0$. These bimagnon peaks are very reminiscent of quantum scars in nonintegrable systems [47–50], where ladders of scar states in nonintegrable one-dimensional spin systems have been shown to be generated from any single member of the set through the action of two-particle operators. We believe that states corresponding to our bimagnon peaks do not represent scars because of the projective measurements performed to reach there, and moreover, unlike the topological entanglement entropy of typical Kitaev states which are of the order of $\ln 2$, here γ is measurably much smaller.

ACKNOWLEDGMENTS

The authors acknowledge support of the Department of Atomic Energy, Government of India, under Project Identification No. RTI 4002, and the Department of Theoretical Physics, TIFR, for computational resources.

-
- [1] A. Lavasani, Z.-X. Luo, and S. Vijay, *Phys. Rev. B* **108**, 115135 (2023).
 - [2] A. Sriram, T. Rakovszky, V. Khemani, and M. Ippoliti, *Phys. Rev. B* **108**, 094304 (2023).
 - [3] T.-C. Lu, L. A. Lessa, I. H. Kim, and T. H. Hsieh, *PRX Quantum* **3**, 040337 (2022).
 - [4] R. Verresen, N. Tantivasadakarn, and A. Vishwanath, arXiv preprint arXiv:2112.03061 (2021).
 - [5] W.-H. Zhang, C. Zhang, Z. Chen, X.-X. Peng, X.-Y. Xu, P. Yin, S. Yu, X.-J. Ye, Y.-J. Han, J.-S. Xu, G. Chen, C.-F. Li, and G.-C. Guo, *Phys. Rev. Lett.* **125**, 030506 (2020).
 - [6] S. Roy, J. T. Chalker, I. V. Gornyi, and Y. Gefen, *Phys. Rev. Res.* **2**, 033347 (2020).
 - [7] J. F. Steiner and F. von Oppen, *Phys. Rev. Res.* **2**, 033255 (2020).
 - [8] G.-Y. Zhu, N. Tantivasadakarn, A. Vishwanath, S. Trebst, and R. Verresen, *Phys. Rev. Lett.* **131**, 200201 (2023).
 - [9] M. Szyniszewski, A. Romito, and H. Schomerus, *Phys. Rev. Lett.* **125**, 210602 (2020).
 - [10] B. Skinner, J. Ruhman, and A. Nahum, *Phys. Rev. X* **9**, 031009 (2019).
 - [11] O. Lunt and A. Pal, *Phys. Rev. Res.* **2**, 043072 (2020).
 - [12] Y. Bao, S. Choi, and E. Altman, *Phys. Rev. B* **101**, 104301 (2020).
 - [13] S. Choi, Y. Bao, X.-L. Qi, and E. Altman, *Phys. Rev. Lett.* **125**, 030505 (2020).
 - [14] S. Czischek, G. Torlai, S. Ray, R. Islam, and R. G. Melko, *Phys. Rev. A* **104**, 062405 (2021).
 - [15] A. Chan, R. M. Nandkishore, M. Pretko, and G. Smith, *Phys. Rev. B* **99**, 224307 (2019).
 - [16] M. Szyniszewski, A. Romito, and H. Schomerus, *Phys. Rev. B* **100**, 064204 (2019).
 - [17] C.-M. Jian, Y.-Z. You, R. Vasseur, and A. W. W. Ludwig, *Phys. Rev. B* **101**, 104302 (2020).
 - [18] Y. Li, X. Chen, and M. P. A. Fisher, *Phys. Rev. B* **98**, 205136 (2018).

- [19] E. Tirrito, A. Santini, R. Fazio, and M. Collura, *SciPost Phys.* **15**, 096 (2023).
- [20] T. Minato, K. Sugimoto, T. Kuwahara, and K. Saito, *Phys. Rev. Lett.* **128**, 010603 (2022).
- [21] M. Block, Y. Bao, S. Choi, E. Altman, and N. Y. Yao, *Phys. Rev. Lett.* **128**, 010604 (2022).
- [22] T. Müller, S. Diehl, and M. Buchhold, *Phys. Rev. Lett.* **128**, 010605 (2022).
- [23] M. J. Gullans and D. A. Huse, *Phys. Rev. X* **10**, 041020 (2020).
- [24] S. Vijay, arXiv preprint arXiv:2005.03052 (2020).
- [25] S. Sahu, S.-K. Jian, G. Bentsen, and B. Swingle, *Phys. Rev. B* **106**, 224305 (2022).
- [26] G. S. Bentsen, S. Sahu, and B. Swingle, *Phys. Rev. B* **104**, 094304 (2021).
- [27] G. Kells, D. Meidan, and A. Romito, *SciPost Phys.* **14**, 031 (2023).
- [28] A. Kitaev, *Annals of Physics* **321**, 2 (2006), january Special Issue.
- [29] A. Kitaev and J. Preskill, *Phys. Rev. Lett.* **96**, 110404 (2006).
- [30] M. Gohlke, R. Moessner, and F. Pollmann, *Phys. Rev. B* **98**, 014418 (2018).
- [31] S. Kumar, S. Sharma, and V. Tripathi, *Phys. Rev. B* **104**, 245113 (2021).
- [32] K. Satzinger, Y.-J. Liu, A. Smith, C. Knapp, M. Newman, C. Jones, Z. Chen, C. Quintana, X. Mi, A. Dunsworth, *et al.*, *Science* **374**, 1237 (2021).
- [33] M. Coppola, E. Tirrito, D. Karevski, and M. Collura, *Phys. Rev. B* **105**, 094303 (2022).
- [34] D. Rossini and E. Vicari, *Phys. Rev. B* **102**, 035119 (2020).
- [35] O. Alberton, M. Buchhold, and S. Diehl, *Phys. Rev. Lett.* **126**, 170602 (2021).
- [36] Y. Li, X. Chen, and M. P. A. Fisher, *Phys. Rev. B* **100**, 134306 (2019).
- [37] T. Brydges, A. Elben, P. Jurcevic, B. Vermersch, C. Maier, B. P. Lanyon, P. Zoller, R. Blatt, and C. F. Roos, *Science* **364**, 260 (2019).
- [38] K. L. Hur, *Annals of Physics* **323**, 2208 (2008).
- [39] X.-L. Wang, Q.-L. Yue, C.-H. Yu, F. Gao, and S.-J. Qin, *Scientific Reports* **7**, 12122 (2017).
- [40] A. Valdés-Hernández, A. P. Majtey, and A. R. Plastino, *Phys. Rev. A* **91**, 032313 (2015).
- [41] M. Gärttner, P. Hauke, and A. M. Rey, *Phys. Rev. Lett.* **120**, 040402 (2018).
- [42] D. Bussandri, A. P. Majtey, and A. Valdés-Hernández, *Journal of Physics A: Mathematical and Theoretical* **53**, 405303 (2020).
- [43] P. Weinberg and M. Bukov, *SciPost Phys.* **2**, 003 (2017).
- [44] P. Weinberg and M. Bukov, *SciPost Phys.* **7**, 020 (2019).
- [45] G. Piccitto, A. Russomanno, and D. Rossini, *Phys. Rev. B* **105**, 064305 (2022).
- [46] T.-C. Lu, T. H. Hsieh, and T. Grover, *Phys. Rev. Lett.* **125**, 116801 (2020).
- [47] M. Schecter and T. Iadecola, *Phys. Rev. Lett.* **123**, 147201 (2019).
- [48] S. Moudgalya, S. Rachel, B. A. Bernevig, and N. Regnault, *Phys. Rev. B* **98**, 235155 (2018).
- [49] S. Moudgalya, N. Regnault, and B. A. Bernevig, *Phys. Rev. B* **98**, 235156 (2018).
- [50] T. Iadecola, M. Schecter, and S. Xu, *Phys. Rev. B* **100**, 184312 (2019).